

Engineering Notes

ENGINEERING NOTES are short manuscripts describing new developments or important results of a preliminary nature. These Notes cannot exceed 6 manuscript pages and 3 figures; a page of text may be substituted for a figure and vice versa. After informal review by the editors, they may be published within a few months of the date of receipt. Style requirements are the same as for regular contributions (see inside back cover).

Optimal Simultaneous Pairwise Conflict Resolution Maneuvers in Air Traffic Management

John C. Clements*
Dalhousie University,
Halifax, Nova Scotia B3H 3J5, Canada

I. Introduction

ONE objective of immediate interest to the air traffic management community is the development of automatic monitoring and guidance systems for the detection and resolution of conflicting aircraft trajectories. In part, this is directed toward the recently proposed free-flight or user-preferred trajectories environment,¹ but there is also an important role for such systems as a supplementary backup to standard air traffic control and planning operations at busy airports and in congested control zones.^{2–4} Although the pairwise collision avoidance/conflict resolution problem is only one small aspect of an overall management program, it is likely to form a basic component of such a system. Numerous approaches to this problem have been considered. For a description of the problem, as well as a detailed analysis of some of the most recent advances, the reader is referred to Refs. 2–7. Kuchar and Yang⁸ also provide a comprehensive survey of conflict detection and resolution models.

In this work, we consider two aircraft traversing potentially conflicting planar trajectories (cf. Fig. 1a). The conflict detection and resolution algorithm developed here is velocity-vector-based with the avoidance maneuvers executed at constant airspeed in the horizontal plane. For simplicity, the performance objective incorporated into the optimal control formulation of the problem is to minimize the time during which both aircraft are deviated from their respective nominal ground tracks. Because trajectories are flown at constant airspeed, this minimum-time deviation objective is equivalent to a minimum-distance deviation, provided the distance is interpreted as the length of the flight path from the fixed point of departure to the (first possible) point of return to the aircraft's nominal ground track and heading. When a potential conflict is detected, optimal simultaneous avoidance maneuvers are computed that preserve aircraft separation. The form of the optimal control history is determined from an analysis of the associated Hamiltonian and costate equations, and the algorithm is then formulated to yield solutions possessing the same structure. Consideration of alternative objectives based on aircraft operating efficiency and/or user-preferred options would be important in any practical implementation of the approach developed here.

The key constraint in the formulation of the problem is Eq. (3), which specifies the minimum separation distance permitted during execution of the avoidance maneuvers, with, for example, $r_s =$

5 n mile. The minimum-time trajectories around such a constraint may not themselves be candidates for practical conflict resolution, but rather define the inner envelope of all possible constant-air-speed avoidance maneuvers. That is, if an avoiding aircraft crosses the minimum-time trajectory at any point, then the mandatory aircraft separation condition is violated and additional evasive maneuvers will be required. However, minimum-time trajectories satisfying a multiple, for example, 1.5, of the mandatory separation distance could provide information regarding advisory safe flight trajectories. In Ref. 9, the conflict scenarios were considered noncooperative, with the first aircraft traveling at constant airspeed v_1 and direction throughout the execution of the avoidance maneuver by the second aircraft, which was constrained to maneuver at constant airspeed v_2 . Clearly, the total minimum-time deviation from the nominal flight

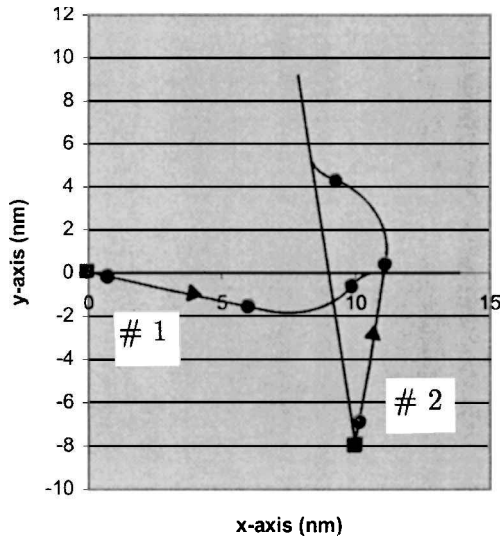


Fig. 1a Optimal trajectories for example 1 ($\bullet, t_{i,j}$); nm, nautical miles.

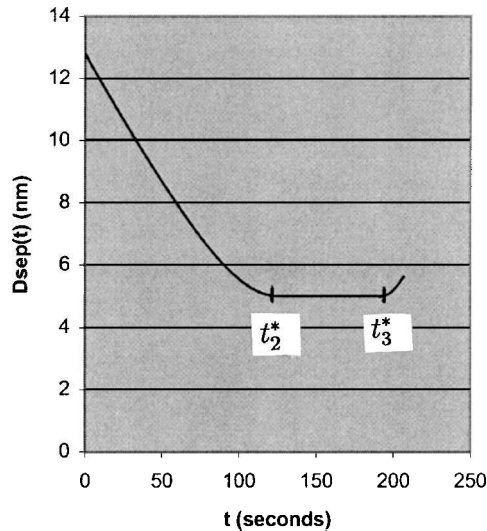


Fig. 1b Separation distance $D_{sep}(t)$ for example 1 (with times t_2^*, t_3^*); nm, nautical miles.

Received 19 January 2001; revision received 16 July 2001; accepted for publication 8 February 2002. Copyright © 2002 by John C. Clements. Published by the American Institute of Aeronautics and Astronautics, Inc., with permission. Copies of this paper may be made for personal or internal use, on condition that the copier pay the \$10.00 per-copy fee to the Copyright Clearance Center, Inc., 222 Rosewood Drive, Danvers, MA 01923; include the code 0731-5090/02 \$10.00 in correspondence with the CCC.

*Professor, Department of Mathematics and Statistics.

tracks could be improved with the execution of simultaneous cooperative maneuvering by both aircraft, and it is this option that is addressed here. The optimal control problem is described in Sec. II. Solutions require the calculation of the boundary arc control law,⁹ that is, the precise steering programs for the time interval when the separation constraint is satisfied exactly. In Sec. III, a simple, robust time-stepping algorithm is derived that will detect potential conflicts and compute minimum-time avoidance maneuvers for both aircraft in real time. An example application is considered in Sec. IV, and the results are displayed in Fig. 1. In Fig. 1a, the optimal avoidance trajectories are given by the solid curves (with direction arrows) where the solid boxes specify the initial positions (a_1, b_1) and (a_2, b_2) of aircraft 1 and 2, the solid straight lines indicate the nominal ground tracks, and the solid dots indicate the switching times t_i of the turn rate control of each aircraft. As is shown in Fig. 1b, the algorithm maintains the minimum separation between the maneuvering aircraft.

II. Problem Formulation

The optimal control problem in a fixed xy Cartesian coordinate system is to determine the steering programs $\chi_i^*(t)$, $0 \leq t \leq t_{i,f}^*$, $i = 1, 2$ that guide aircraft 1 and 2 along those planar trajectories $C_i^* := \{[x_i^*(t), y_i^*(t)] | 0 \leq t \leq t_{i,f}^*, x_i^*, y_i^* \in C^1[0, t_{i,f}^*]\}$, $i = 1, 2$, that reacquire their respective nominal ground track trajectories in minimum time without violating the specified separation constraint. This minimal separation distance is denoted by r_s in Eq. (3). The airspeeds v_1 and v_2 of each aircraft are assumed to remain constant throughout the avoidance maneuvers. The control functions $u_i(t)$, $i = 1, 2$, are the turn rates of each aircraft, and the control variable constraints are defined in terms of the maximum allowable turn rates $|u_i(t)| \leq u_{Mi}$, $0 \leq t \leq t_{i,f}$, $i = 1, 2$, which can be employed at any point during the execution of the avoidance maneuver. Here, $u_i(t) = u_{Mi}$ corresponds to a maximum allowable rate of turn to the left and $u_i(t) = -u_{Mi}$ to a maximum rate turn to the right. These turn rate constraints are those normally associated with passenger safety and comfort, although there is certainly the possibility of replacing them with values that could correspond to an emergency response. The dynamics are formulated in terms of the state equations,

$$\begin{aligned} \dot{x}_i(t) &= v_i \cos \chi_i(t), & \dot{y}_i(t) &= v_i \sin \chi_i(t), & \dot{\chi}_i(t) &= u_i(t) \\ 0 &\leq t \leq t_{i,f}, & i &= 1, 2 \end{aligned} \quad (1)$$

the control constraints,

$$|u_i(t)| \leq u_{Mi}, \quad 0 \leq t \leq t_{i,f}, \quad i = 1, 2 \quad (2)$$

the state variable constraints,

$$\begin{aligned} g[x_1(t), y_1(t), x_2(t), y_2(t)] &= r_s^2 - [x_1(t) - x_2(t)]^2 \\ &- [y_1(t) - y_2(t)]^2 \leq 0, \quad 0 \leq t \leq \max\{t_{i,f}\} \end{aligned} \quad (3)$$

the initial conditions,

$$\begin{aligned} t = 0: x_1(0) &= a_1, & y_1(0) &= b_1, & \chi_1(0) &= \chi_{1o} \\ x_2(0) &= a_2, & y_2(0) &= b_2, & \chi_2(0) &= \chi_{2o} \end{aligned} \quad (4)$$

and the end conditions for a return to the nominal ground tracks,

$$\begin{aligned} t &= t_{i,f}: \chi_i(t_{i,f}) = \chi_{io} \\ y_i(t_{i,f}) &= \tan(\chi_{io})[x_i(t_{i,f}) - a_i] + b_i, \quad i = 1, 2 \end{aligned} \quad (5)$$

The constants $\{(a_1, b_1), (a_2, b_2), \chi_{1o}, \chi_{2o}\}$ define the initial positions and nominal ground tracks for aircraft 1 and 2 and, together with v_1 and v_2 , completely determine any potential conflict configuration. A potential conflict is said to exist at time $t = 0$ if the separation constraint (3) will be violated at some future time $t > 0$, unless one or both aircraft execute an avoidance maneuver. In what follows, a subarc of a feasible trajectory C_i for which $g[x_1(t), y_1(t), x_2(t), y_2(t)] < 0$ in Eq. (3) will be called an interior arc and a subarc for which $g[x_1(t), y_1(t), x_2(t), y_2(t)] = 0$ will be

termed a boundary arc. The Hamiltonian for the problem defined by Eqs. (1–5) is given by

$$\begin{aligned} H(t) &= -1 + \lambda^T f + \mu(t)[\nabla g]^T f \\ &= -1 + \lambda_1(t)v_1 \cos \chi_1(t) + \lambda_2(t)v_1 \sin \chi_1(t) + \lambda_3(t)u_1(t) \\ &\quad + \lambda_4(t)v_2 \cos \chi_2(t) + \lambda_5(t)v_2 \sin \chi_2(t) + \lambda_6(t)u_2(t) \\ &\quad - 2\mu(t)[x_1(t)v_1 \cos \chi_1(t) - y_1(t)v_1 \sin \chi_1(t) \\ &\quad + x_2(t)v_2 \cos \chi_2(t) - y_2(t)v_2 \sin \chi_2(t)] \end{aligned} \quad (6)$$

where $\mu(t) = 0$ on interior arcs of trajectories and the Lagrange multipliers $\lambda_i(t)$ satisfy the following costate equations:

$$\begin{aligned} \dot{\lambda}_1(t) &= -\frac{\partial H}{\partial x_1} = 2\mu(t)v_1 \cos \chi_1(t) \\ \dot{\lambda}_2(t) &= -\frac{\partial H}{\partial y_1} = -2\mu(t)v_1 \sin \chi_1(t) \\ \dot{\lambda}_3(t) &= -\frac{\partial H}{\partial \chi_1} = \lambda_1(t)v_1 \sin \chi_1(t) - \lambda_2(t)v_1 \cos \chi_1(t) \\ &\quad - 2\mu(t)v_1[x_1(t) \sin \chi_1(t) - y_1(t) \cos \chi_1(t)] \\ \dot{\lambda}_4(t) &= -\frac{\partial H}{\partial x_2} = 2\mu(t)v_2 \cos \chi_2(t) \\ \dot{\lambda}_5(t) &= -\frac{\partial H}{\partial y_2} = -2\mu(t)v_2 \sin \chi_2(t) \\ \dot{\lambda}_6(t) &= -\frac{\partial H}{\partial \chi_2} = \lambda_3(t)v_2 \sin \chi_1(t) - \lambda_4(t)v_2 \cos \chi_2(t) \\ &\quad - 2\mu(t)v_2[x_2(t) \sin \chi_2(t) - y_2(t) \cos \chi_2(t)] \end{aligned} \quad (7)$$

for all t in $[0, t_{i,f}]$ (Ref. 10). By the Pontryagin maximum principle (see Ref. 10), on any interior arcs [where $\mu(t) = 0$] the optimal controls $u_i^*(t)$ must satisfy

$$\begin{aligned} u_i^*(t) &= \begin{array}{ll} -u_{Mi} & \text{for } \lambda_3^*(t) < 0 \text{ if } i = 1 \text{ or } \lambda_5^*(t) < 0 \text{ if } i = 2 \\ \text{undetermined} & \text{for } \lambda_3^*(t) = 0 \text{ if } i = 1 \text{ or } \lambda_5^*(t) = 0 \text{ if } i = 2 \\ u_{Mi} & \text{for } \lambda_3^*(t) > 0 \text{ if } i = 1 \text{ or } \lambda_5^*(t) > 0 \text{ if } i = 2 \end{array} \end{aligned} \quad (8)$$

Intervals of optimal singular control on interior arcs [$\mu(t) = 0$] correspond to values of t for which $\lambda_3^*(t) = 0$ and/or $\lambda_5^*(t) = 0$. If $\mu(t) = 0$ and $\lambda_3^*(t) = 0$ [hence, also $\dot{\lambda}_3^*(t) = 0$], then from Eq. (7), $\lambda_1^*(t)$ and $\lambda_2^*(t)$ must be constant and $\dot{\lambda}_3^*(t) = \lambda_1^*(t)v_1 \sin \chi_1^*(t) - \lambda_2^*(t)v_1 \cos \chi_1^*(t) = 0$. For this to be true, however, $\chi_1^*(t)$ must be constant, which means that the optimal singular control for aircraft 1 is $u_1^*(t) = 0$, that is, straight flight. An identical argument yields the optimal singular control [$u_2^*(t) = 0$] for aircraft 2. Hence, except on a boundary arc [$\mu(t) \neq 0$ and $g = 0$], each optimal control corresponds to either a maximum performance turn or straight flight. If straight flight rather than a maximum performance turn is executed initially by either aircraft, then that trajectory cannot be a path of minimum distance unless no evasive maneuver was required in the first place. If more than one turn is executed by either aircraft before interception with the boundary arc, then, again, the trajectory cannot be a path of minimum distance. Thus, optimal trajectories must begin with a single maximum performance turn, followed by straight flight to the interception point corresponding to boundary arc control. The feasible extremal control histories are defined in terms of switching times $t_{i,j}^*$, $i = 1, 2, j = 1, 2, \dots$, and there can only be four possible candidates for feasible extremals for any conflict configuration. That is, if a potential conflict exists, then the four candidates correspond to the four possible first turn sequences [right–right (RR) (i.e., initial right turn for aircraft 1 and initial right turn for aircraft 2), right–left (RL), left–right (LR), or left–left (LL)] and each must have a control history of the following form: 1) a maximum rate turn [$u_i^*(t) = \rho_i u_{Mi}$,

$\rho_i = \pm 1$, $0 \leq t \leq t_{i,1}^*$, $i = 1, 2$] to those radials $[u_i^*(t) = 0, t_{i,1}^* \leq t \leq t_{i,2}^*]$, $t_{1,2}^* = t_{2,2}^*$ that intercept the boundary arc defined by Eq. (3), followed by 2) flight along the boundary arc trajectories for time $t_{i,2}^* \leq t \leq t_{i,3}^*$, $i = 1, 2$, $t_{1,3}^* = t_{2,3}^*$, followed by 3) a final radial $[u_i^*(t) = 0, t_{i,3}^* \leq t \leq t_{i,4}^*]$ and a maximum performance opposite turn $[u_i^*(t) = -\rho_i u_{Mi}, \rho_i = \pm 1, t_{i,4}^* \leq t \leq t_{i,f}^* = t_f^*, i = 1, 2]$ back to the nominal ground track trajectory of each aircraft (cf. Fig. 1a).

Because the boundary arc control corresponds to a mutual separation of exactly r_s , the entry times to, and exit times from, this control must be the same for both aircraft. That is, $t_{1,2}^* = t_{2,2}^*$ and $t_{1,3}^* = t_{2,3}^*$. Moreover, the final time of interception with their respective nominal ground tracks must also be the same for both aircraft, that is, $t_{i,f}^* = t_f^*$, $i = 1, 2$. This last result is an immediate consequence of the observation that if one of the final times is greater, the first switching times $t_{1,1}^*$ and $t_{2,1}^*$ can always be adjusted to eliminate that difference. The times $t_{i,4}^*$, $i = 1, 2$ depend on the positions of each aircraft relative to their nominal ground tracks once they exit the interval of boundary arc control. In those cases where a final straight radial is not required as part of the maneuver, we simply set $t_{i,4}^* = t_{i,3}^*$.

The precise form of the boundary arc control is extremely difficult to determine in the case of simultaneous avoidance maneuvering and, as is shown in the example application in Sec. IV, this control is normally in effect for a significant portion of the avoidance maneuver. In Ref. 9, a moving reference frame centered on aircraft 1 was introduced. That approach worked well because the trajectory of aircraft 1 was known a priori, and the precise form of the boundary arc control law could be derived analytically in terms of a differential-algebraic system of equations. In the case of simultaneous maneuvers, this same approach would require an iterative solution procedure in which, alternately, one trajectory is fixed and the second computed until a mutually optimum solution is achieved. Such a solution program is clearly outside any real-time computational objective, although it does provide a means of verifying solutions obtained using alternate algorithms. In the next section, we derive a very simple algorithm that computes accurate optimal simultaneous avoidance maneuvers in real time and recovers all of the boundary arc control history.

III. Solution Algorithm

At any fixed instant of time during the flight maneuvers by both aircraft, that is, for any given values of the position and heading variables of aircraft 1 and 2, for example, $\{\alpha_1, \beta_1, \alpha_2, \beta_2, \chi_1, \chi_2\}$ (which will be different from the initial values a_1, b_1, χ_{10} , etc.), the separation distance $D(t)$ between the two aircraft satisfies

$$D^2(t) = \{[\alpha_1 + t v_1 \cos(\chi_1)] - [\alpha_2 + t v_2 \cos(\chi_2)]\}^2 + \{[\beta_1 + t v_1 \sin(\chi_1)] - [\beta_2 + t v_2 \sin(\chi_2)]\}^2$$

Because

$$\ddot{D}^2(t) = 2[v_1 \cos(\chi_1) - v_2 \cos(\chi_2)]^2 + 2[v_1 \sin(\chi_1) - v_2 \sin(\chi_2)]^2 > 0$$

for all $t > 0$, $D(t)$ has a unique global minimum at time

$$T_{\min} = -A/B \quad (9)$$

where

$$A = 2\alpha_1 v_1 \cos(\chi_1) - 2\alpha_1 v_2 \cos(\chi_2) - 2\alpha_2 v_1 \cos(\chi_1) + 2\alpha_2 v_2 \cos(\chi_2) + 2\beta_1 v_1 \sin(\chi_1) - 2\beta_1 v_2 \sin(\chi_2) - 2\beta_2 v_1 \sin(\chi_1) + 2\beta_2 v_2 \sin(\chi_2) \quad (10)$$

$$B = 2v_1^2 \cos^2(\chi_1) - 4v_1 \cos(\chi_1)v_2 \cos(\chi_2) + 2v_2^2 \cos^2(\chi_2) + 2v_1^2 \sin^2(\chi_1) - 4v_1 \sin(\chi_1)v_2 \sin(\chi_2) + 2v_2^2 \sin^2(\chi_2) \quad (11)$$

and this global minimum separation distance D_{\min} is given by

$$D_{\min} = \{[\alpha_1 - A v_1 \cos(\chi_1)/B - \alpha_2 + A v_2 \cos(\chi_2)/B]^2 + [\beta_1 - A v_1 \sin(\chi_1)/B - \beta_2 + A v_2 \sin(\chi_2)/B]^2\}^{1/2} \quad (12)$$

with A and B as in Eqs. (10) and (11). Both the initial radial to the boundary arc and the boundary arc control law are determined as a

time-stepping sequence of straight flight and attempted maximum rate turns (as described in steps 3 and 4 hereafter), which avoid violating the constraint $D_{\min} \geq r_s$. This sequence is continued until that radial normal to the nominal flight track is acquired (at which time straight flight, followed by a maximum rate opposite turn, is executed) or until a maximum rate opposite turn alone would acquire the nominal flight track. The algebraic equations required to identify and compute these final radials and maximum performance opposite turns (step 4 of the algorithm presented hereafter) require the straightforward determination of points of intersection of radial vectors with turn circles of fixed radius and are described in detail in Sec. IV of Ref. 9. The distance separating the two aircraft at any time $t \geq 0$ is $D_{\text{sep}}(t) = \{[x_1(t) - x_2(t)]^2 + [y_1(t) - y_2(t)]^2\}^{1/2}$. These simple observations, together with the required structure of the control history on interior arcs (8), is the basis of the following real-time solution algorithm that, in the interest of brevity, is given here in a somewhat literal context. When a potential conflict configuration exists (i.e., $D_{\min} < r_s$ at time $t = 0$), the following steps produce the four feasible extremal candidates for the simultaneous avoidance maneuvers. The one requiring least time is the optimal solution. Recall that at any time t , D_{\min} is the minimum separation distance between the two aircraft that would occur if they continued to fly straight on their respective ground headings, whereas $D_{\text{sep}}(t)$ is the distance separating the two aircraft at time t .

Algorithm: for each feasible extremal candidate (RR, RL, LR, and LL).

1) Set the incremental time step Δt .

2) In increments of time Δt , both aircraft execute maximum rate turns $[u_i^*(t) = \rho_i u_{Mi}, \rho_i = \pm 1]$ in the directions specified by the extremal candidate, for example, RR, until $D_{\min} = r_s$ is satisfied, that is, for time $t_{1,1}^* = t_{2,1}^* = t_1^*$. Note that for this first approximation, the switching times $t_{1,1}^*$ and $t_{2,1}^*$ are necessarily equal because the same increment has been added at each time step for the same number of steps. These times are later modified in step 5 after information regarding the final times has become available.

3) At each subsequent time step, both aircraft attempt to execute maximum rate turns for time Δt back to their respective nominal ground tracks, that is, $u_i^*(t) = -\rho_i u_{Mi}$. If $D_{\min} < r_s$ would result from such turns executed at any step, then both aircraft continue to fly straight, that is, $u_i^*(t) = 0$, during that time step. Otherwise, both execute maximum rate turns toward their nominal ground tracks for time Δt . Note that $t_{1,2}^* = t_{2,2}^* = t_2^*$ is that time when the actual aircraft separation $D_{\text{sep}}(t)$ first equals r_s . This step will produce straight radials to the interception point of the boundary arc, followed by a curved path along the boundary arc, that is, the boundary arc turn, as indicated in Fig. 1b.

4) Step 3 continues until that time $t_{1,3}^* = t_{2,3}^* = t_3^*$ (if it exists) when a straight radial $[u_i^*(t) = 0, t_{i,3}^* \leq t \leq t_{i,4}^*, i = 1, 2]$ normal to the nominal ground track trajectory together with a maximum rate opposite turn (or just a maximum rate opposite turn alone, as in Fig. 1a), that is, $u_i^*(t) = \rho_i u_{Mi}$, $t_{i,4}^* \leq t \leq t_{i,f}^*, i = 1, 2$, will result in each aircraft intercepting their respective nominal ground tracks by satisfying Eq. (5). If such a time does not occur, then the particular extremal being executed is not feasible. Because each aircraft is turning away from the constraint set, both $D_{\min} > r_s$ and $D_{\text{sep}}(t) > r_s$ are satisfied for $t_{i,3}^* \leq t \leq t_{i,f}^*, i = 1, 2$.

5) If $t_{1,f}^* > t_{2,f}^*$, then decrease $t_{1,1}^*$ and increase $t_{2,1}^*$ by Δt and repeat steps 3 and 4. If $t_{1,f}^* < t_{2,f}^*$, then increase $t_{1,1}^*$ and decrease $t_{2,1}^*$ by Δt and repeat steps 3 and 4. Continue this process until the final times are equal (at least to within a tolerance of time Δt).

Note that, if a potential conflict does not exist, that is, $D_{\min} \geq r_s$ at time $t = 0$, then the algorithm yields the default controls $u_i^*(t) = 0$, $i = 1, 2$, $t > 0$, as expected. The final radial $[u_i^*(t) = 0, t_{i,3}^* \leq t \leq t_{i,4}^*, i = 1, 2]$ (if necessary) must be normal to the respective nominal ground track to preserve the minimum-time (distance) property of the trajectory. In the next section, the algorithm is implemented for an example conflict configuration. For practical reasons, the time step chosen for the example is $\Delta t = 0.25$ s. Much smaller values could be chosen without substantially affecting computation times, but would not necessarily reflect realistic time frames required to execute a change in directional control.

IV. Example Application

Distances and positions are measured in nautical miles from a fixed origin in the xy plane. Steering (heading) angles χ are measured in degrees, anticlockwise from the positive x axis. The units of time and speed are hours and knots, respectively. The maximum allowable turn rates u_{M_i} are given in degrees per second and are consistent with standard rate turns at the speeds chosen for this example. To provide a basis for comparison, the example conflict configuration chosen here is same configuration as that considered in Ref. 9, except that, in that study, only one aircraft executed the avoidance maneuver at a time. The data for the example conflict avoidance configuration are shown in example 1:

$$\{(a_1, b_1), (a_2, b_2), \chi_{10}, \chi_{20}, v_1, v_2, u_{M1}, u_{M2}, r_s\} \\ = \{(0, 0), (10, -8), 0.0, 97.15, 200, 250, 2.86, 2.86, 5\} \quad (13)$$

The output required for the optimal control and display of the conflict resolution maneuvers are the switching times $t_{i,j}^*$, which were computed to within an error tolerance of 0.25 s for each feasible extremal using $\Delta t = 0.25$ s. In example 1, the optimal solution is the RR feasible extremal requiring 207.25 s to execute. The switching times were computed to be (in seconds)

$$t_{1,1}^* = 5.75, \quad t_{2,1}^* = 5.25, \quad t_{1,2}^* = t_{2,2}^* = 126.5 \\ t_{1,3}^* = t_{2,3}^* = 191.0, \quad t_{1,f}^* = t_{2,f}^* = 207.25$$

Only one iteration of step 5 in the algorithm was necessary. Because no final radials were required for the optimal extremals (i.e., $t_{i,4}^* = t_{i,3}^*$, $i = 1, 2$ in step 4 of the algorithm), t_4^* is not included here. The plots of the optimal trajectories are given in Fig. 1a. Figure 1b illustrates the 64.5 s of boundary arc control. A comparison of the results for example 1 considered here with those obtained for (the same initial configuration) examples 1c and 1d in Ref. 9 show that permitting simultaneous cooperative maneuvering can reduce path deviation times considerably (in this case, to 207.25 s from 254.1 s), can yield entirely different optimal trajectories (cf. Ref. 9, where the initial left turn by aircraft 2 proved optimal), and can substantially reduce the extent of the total deviation from the nominal ground tracks. Finally, numerical experiments were carried out to verify that the algorithm derived here (with the additional constraint that only one aircraft executes the avoidance maneuver) reproduces the analytical results obtained for example 1 in Ref. 9.

V. Conclusions

In Sec. III, a simple time-stepping algorithm was presented that will detect potential conflicts and resolve them by computing the globally optimal steering programs for both aircraft in real time. The algorithm is robust because at each time step the procedure verifies that the separation constraint is satisfied. Furthermore, the algorithm accurately recovers all of the boundary arc control history, which, as is shown in the example application in Sec. IV, may constitute a significant portion of the optimal avoidance maneuvers. The algorithm was generated using the form of the optimal control law determined from an analysis of the associated Hamiltonian and costate equations. Incorporating multiple conflicts, more general performance measures, as well as variable airspeeds, into the model will be an important consideration for future work. Because of its simplicity, the algorithm derived may prove to be a useful tool in exploring the design of a comprehensive conflict detection and avoidance system.

Acknowledgment

This research was supported by the Natural Sciences and Engineering Research Council of Canada.

References

- 1Lanzer, N., and Jenny, M. T., "Managing the Evolution to Free Flight," *Journal of Air Traffic Control*, 1995, pp. 8–20.
- 2Erzberger, H., "Design Principles and Algorithms for Automated Air Traffic Management," Knowledge-Based Functions in Aerospace Systems, LS-200, AGARD, Nov. 1995.
- 3Denery, D. G., Erzberger, H., Davis, T. J., Green, S. M., and McNally, B. D., "Challenges of Air Traffic Management Research: Analysis, Simulation, and Field Test," AIAA Paper 97-3832, Aug. 1997.

⁴Krozel, J., Mueller, T., and Hunter, G., "Free-Flight Detection and Resolution Analysis," *Proceedings of the AIAA Guidance, Navigation, and Control Conference*, AIAA, Reston, VA, 1996, pp. 1–11.

⁵Tomlin, C., Pappas, G., and Sastry, S., "Conflict Resolution in Air Traffic Management: A Study in Multi-Agent Hybrid Systems," *IEEE Transactions on Automatic Control*, Vol. 43, No. 4, 1998, pp. 509–521.

⁶Zhao, Y. J., and Schultz, R. L., "Deterministic Resolution of Two-Aircraft Conflict in Free Flight," *Proceedings of the AIAA Guidance, Navigation, and Control Conference*, AIAA, Reston, VA, 1997, pp. 469–478.

⁷Menon, P. K., Sweriduk, G. D., and Sridhar, B., "Optimal Strategies for Free-Flight Air Traffic Conflict Resolution," *Journal of Guidance, Control, and Dynamics*, Vol. 33, No. 2, 1999, pp. 202–211.

⁸Kuchar, K. K., and Yang, C. Y., "Survey of Conflict Detection and Resolution Modeling Methods," *Proceedings of the AIAA Guidance, Navigation, and Control Conference*, AIAA, Reston, VA, 1997, pp. 469–478.

⁹Clements, J. C., and Ingalls, B., "An Extended Model for Pairwise Conflict Resolution in Air Traffic Management," *Optimal Control Applications and Methods*, Vol. 20, 1999, pp. 183–197.

¹⁰Hocking, L. M., *Optimal Control: An Introduction to the Theory with Applications*, Oxford Univ. Press, New York, 1991.

Mechanism for Precision Orbit Control with Applications to Formation Keeping

I. Michael Ross*

Naval Postgraduate School,
Monterey, California 93943

Introduction

DETECTING gravitational waves requires a very large baseline (from hundreds to a million kilometers) for an interferometer.^{1,2} Challenged by this extraordinary requirement, a number of astrophysicists have explored various ways to achieve this from an engineering viewpoint. As documented in Refs. 1 and 2, the idea of using three separated spacecraft orbiting in formation to achieve effective structural rigidity (required by the baseline of the interferometer) was suggested in the early 1980s by Faller and Bender. Based on this concept, the laser interferometerspace antenna (LISA) project was proposed to ESA in 1993, resulting in an ESA/NASA project.^{1,2} When the impact of such possible configurations for terrestrial application was recognized, the U.S. Air Force declared in 1995 that a distributed spacecraft system (DSS) flying in formation was one of the key technology areas for the 21st century.³ It is apparent that, since then, a great deal of research has been done on DSS and formation keeping. Of particular note are Refs. 4–6 and the references contained therein. Carter⁴ presents an excellent survey of linearized equations for relative motion between elliptical orbits. Recently, Melton⁵ extended the equations for a state transition matrix by way of a truncated power series in eccentricity. A perspective on these and other analyses as it pertains to formation keeping is presented by Vadali et al.⁶

One of the central technology areas for formation keeping is maintaining the DSS in formation with little or no propellant. In addition, for interferometric measurements, it is necessary to sense and control the distributed system to an effective structural tolerance of the order of a fraction of the wavelength of interest. In this Note, we propose a simple nonpropulsive mechanism to control the orbital position of a spacecraft to such a high precision. Simply stated, the

Received 6 February 2001; revision received 19 November 2001; accepted for publication 20 February 2002. This material is declared a work of the U.S. Government and is not subject to copyright protection in the United States. Copies of this paper may be made for personal or internal use, on condition that the copier pay the \$10.00 per-copy fee to the Copyright Clearance Center, Inc., 222 Rosewood Drive, Danvers, MA 01923; include the code 0731-5090/02 \$10.00 in correspondence with the CCC.

*Associate Professor, Department of Aeronautics and Astronautics, Code: AA/Ro; imross@nps.navy.mil. Associate Fellow AIAA.